A Concentrated Outbreak of Tornadoes, Downbursts and Microbursts, and Implications Regarding Vortex Classification

GREGORY S. FORBES

Department of Meteorology, The Pennsylvania State University, University Park, PA 16802

ROGER M. WAKIMOTO

Department of the Geophysical Sciences, The University of Chicago, Chicago, IL 60637

Reprinted from MONTHLY WEATHER REVIEW, Vol. 111, No. 1, January 1983
American Meteorological Society
Printed in U. S. A.

Reprinted from MONTHLY WEATHER REVIEW, Vol. 111, No. 1, January 1983
American Meteorological Society
Printed in U. S. A.

A Concentrated Outbreak of Tornadoes, Downbursts and Microbursts, and Implications Regarding Vortex Classification

GREGORY S. FORBES

Department of Meteorology, The Pennsylvania State University, University Park, PA 16802

ROGER M. WAKIMOTO

Department of the Geophysical Sciences, The University of Chicago, Chicago, IL 60637

(Manuscript received 6 November 1981, in final form 13 August 1982)

ABSTRACT

A remarkable case of severe weather occurred near Springfield, Illinois on 6 August 1977. Aerial and ground surveys revealed that 17 cyclonic vortices, an anticyclonic vortex, 10 downbursts and 19 microbursts occurred in a limited (20 km × 40 km) area, associated with a bow-shaped radar echo. About half of the vortices appeared to have occurred along a gust front. Some of the others appear to have occurred within the circulation of a mesocyclone accompanying the bow echo, but these vortices seem to have developed specifically in response to localized boundary-layer vorticity generation associated with horizontal and vertical wind shears on the periphery of microbursts. Some of these vortices, and other destructive vortices in the literature, do not qualify as tornadoes as defined in the *Glossary of Meteorology*. A more pragmatic definition of a tornado is suggested.

1. Introduction

A significant research effort in recent years has involved the development of Doppler radar techniques to identify thunderstorms which produce tornadoes. The efforts have been rather successful, identifying the mesocyclone and tornado vortex signatures as indicators of storms which produce major tornadoes (Lemon *et al.*, 1977; Burgess and Devore, 1979). Lemon and Doswell (1979) have described the development of these tornadoes.

Not every tornado which develops is associated with a thunderstorm possessing a mesocyclone signature, however. Burgess and Donaldson (1979) found that several weak and short-lived tornadoes occurred in developing echoes without detectable mesocyclone circulations or supercell characteristics. Later in their lifetimes these echoes developed mesocyclones and strong tornadoes. Weak tornadoes also can form outside of the mesocyclone circulation along the gust front and flanking line of a supercell thunderstorm (Burgess *et al.*, 1977; Brandes, 1978, 1981) and along gust fronts and downbursts from non-supercell thunderstorms (Burgess and Donaldson, 1979; Fujita, 1979; Wilson *et al.*, 1980; Testud *et al.*, 1980). Additionally, weak tornadoes can form under a flanking cloud line behind or to the right of the main cumulonimbus, where radar echoes are weak or absent (Bates, 1968; Barnum *et al.*, 1970; Burgess and Davies-Jones, 1979; Burgess and Donaldson, 1979; Lemon *et al.*, 1980). In this paper we present additional evidence of tornadoes associated with a gust front and with downbursts. We also present evidence which suggests that some tornadoes may be associated with microbursts.

Fujita (1976b) originated the term "downburst" to describe the intense downdraft involved in an airplane crash. In association with damage near the ground, Fujita (1978) defined the downburst as a "strong downdraft inducing an outward burst of damaging winds on or near the ground." Microbursts are small downbursts with horizontal dimensions less than 4 km (Fujita, 1981).

The damage paths of 8 of the 10 downbursts, 18 of the 19 microbursts, and 18 tornadoes which occurred on 6 August 1977 are shown in Fig. 1. The remaining downbursts and microbursts occurred beyond the east and west edges of the figure. The paths were located using techniques described in Section 2. Description of the damage is presented in Sections 3–5. A complete report on this case study (including 40 damage photographs) is given by Forbes and Wakimoto (1978).

The presence or absence of damaging winds was determined essentially unambiguously over the entire region shown in Fig. 1, as the area was extensively covered by 2 m high corn (readily susceptible to damage). The paths of the 18 tornadoes were unmistak-

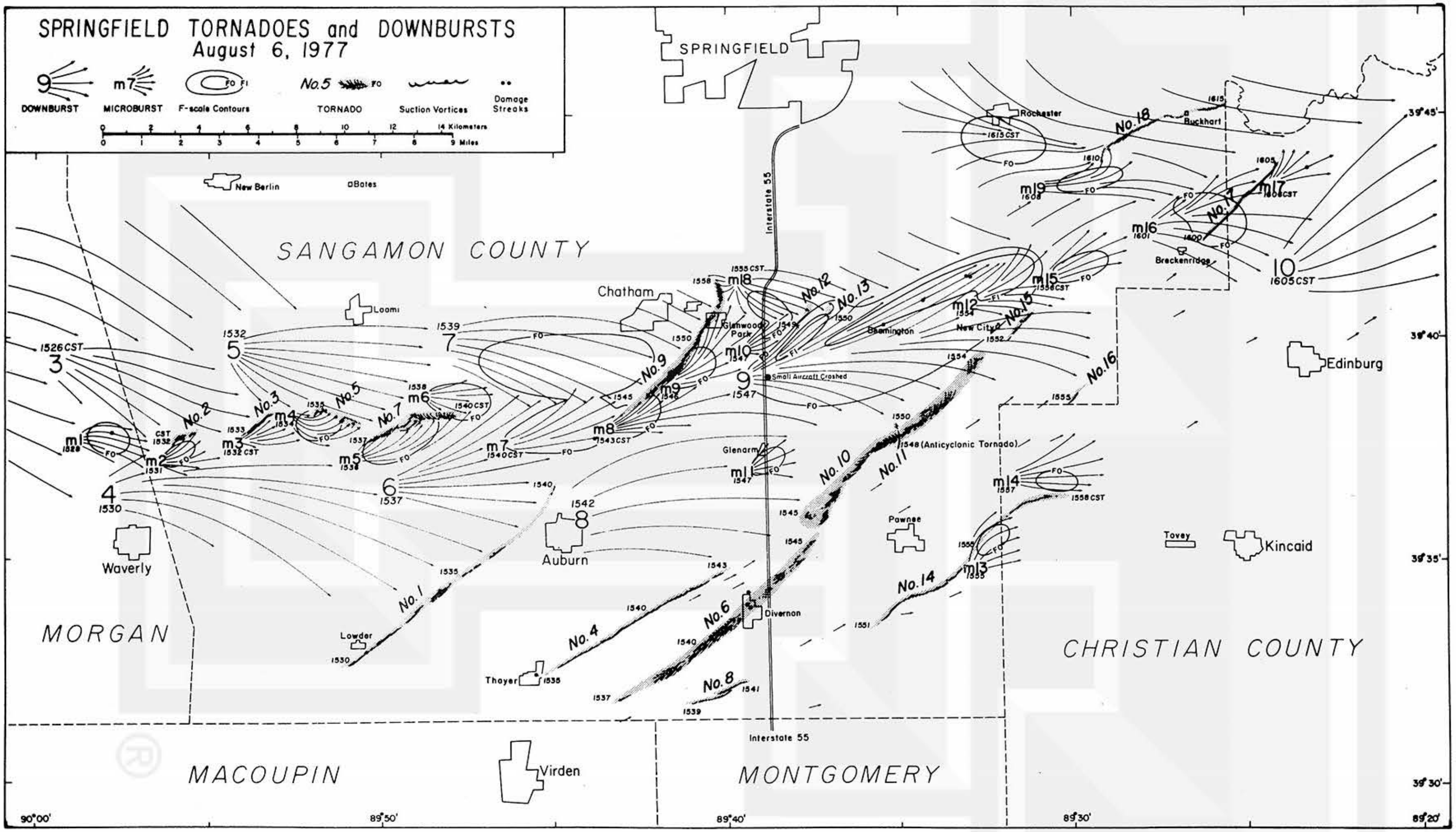

FIG. 1. Mapping of the damage from tornadoes (identified by "No."), downbursts (identified by large numeral), and microbursts (identified by "m") on 6 August 1977. "Streamlines" of damage and F-scale contours are mapped. See figure legend for additional symbol explanation.

ably clear. Thus, it is noteworthy that 18 tornadoes occurred within a 20 km × 40 km area. This tornado density is roughly a factor of 10 greater than that of the 3 April 1974 "super outbreak" (Fujita, 1975). The average spacing between tornadoes 1, 4, 6 and 8 of Fig. 1, occurring essentially simultaneously, was about 4 km, whereas the lateral separation between simultaneously-occurring tornadoes on 3 April 1974 was about 45 km. Clearly, the tornadoes of 6 August 1977 were not part of a typical outbreak of family tornadoes, such as those presented by Fujita *et al.* (1970), Fujita (1974) and Galway (1981). In fact, the density of vortex occurrences on 6 August 1977 raises some questions about the criteria for tornado classification. These criteria are discussed in Section 6.

2. Techniques for classifying damage from tornadoes, downbursts and microbursts

Damaging wind speeds on 6 August 1977 were estimated using the Fujita (1973) scale, referred to as F-scale. Fujita (1981) presents details of the estimation of F-scale on the basis of damage to trees, vehicles and structures. For example, F0 (18–32 m s^{-1}) winds produce some damage to chimneys, antennas, billboards and tree branches. A few shallow-rooted trees may be uprooted. F1 (33–49 m s^{-1}) winds normally damage roofs, overturn mobile homes and uproot trees. Some trees may be snapped. Once winds reach F3 category (70–92 m s^{-1}), roofs are removed and some walls are torn off well-constructed frame homes, and most trees are uprooted or snapped.

Tornado path lengths and path widths were based upon the extent of the F0 damage. Scales for path length and average path width were assigned using the Pearson scales (Fujita, 1973). All reported tornadoes are now rated by the National Severe Storms Forecast Center using these Fujita and Pearson scales, the FPP scheme (Kelly *et al.*, 1978).

Wind speeds deduced on the basis of damage appearance must be considered only estimates of the true wind speed. There are many inherent limitations in the technique due to variables which include housing construction practices, building orientation, duration of wind required to damage various structures, and, in the case of trees and other vegetation-species, upwind fetch, and soil moisture and type. Nevertheless, engineering-oriented examinations of tornado damage by Minor *et al.* (1977) indicate that F-scale estimates of wind speed based upon damage appearance are accurate at winds below about 55 m s^{-1}, but are less reliable at wind speeds which produce more extensive damage (appearing to be F4 of F5). Fujita and Wakimoto (1981) discuss wind speed estimation techniques in additional detail.

When damaging winds occur away from trees and structures, other techniques must be used. Some of these are based upon experience gained during past damage surveys performed by the authors, studies by Fujita (1978), and discussions with farmers and agriculture experts. A rule of thumb invoked during the 6 August 1977 surveys was that some corn is damaged by winds at the low end of the F0 category (~20 m s^{-1}), and damage becomes extensive as the winds approach F1.

If the tornado path contains suction vortex swaths, then the speed of revolution of suction vortices about the tornado axis can be estimated from the swath shape, if the speed of tornado translation U can be estimated. Using the technique presented by Fujita *et al.* (1970), the shape of the swath (cycloid) determines the ratio of revolution and translation velocities, VU^{-1}. The maximum wind speed occurs on the right side of the tornado (facing in the direction toward which the tornado is translating) and is approximately $V + U$, neglecting radial velocity and neglecting the speed of winds rotating about the axis of the suction vortex. Forbes (1978) calculated speeds of rotation averaging 39 m s^{-1} in well-developed suction vortices, however. Thus, total wind speed may exceed $V + U$ by more than 39 m s^{-1}.

Tornado 9 was classified as F3, on the basis of both damage to structures and the shape of looping marks in the suction swath patterns. These loops were more broad and more pronounced than in any of the other tornadoes, and suggested that $VU^{-1} \approx 3$. With a translation speed of about 15 m s^{-1} and the rotation about the suction vortex axis estimated at 20 m s^{-1}, the maximum wind speed in tornado 9 was estimated as 80 m s^{-1} (sum of translation, revolution and suction vortex rotation). Looping marks in suction swaths observed by the authors on other occasions suggest that VU^{-1} can be as large as 3 or 4 in tornadoes translating 20 m s^{-1} or slightly faster. Thus, extreme structural damage is not necessary for categorizing a tornado as F4 or even F5, though present tornado statistics certainly contain that classification bias.

In the absence of suction vortex swaths, easterly components of damaging winds signify strong tangential velocities in a tornado moving eastward. On the left (north) side of the tornado path the total wind speed is $V - U$ because the translational and tangential velocities are in opposite directions. To produce crop damage the winds here must be ~20 m s^{-1} or stronger (using the rule of thumb mentioned above). Hence, if U = 15 m s^{-1}, V must be at least 35 m s^{-1}. For an axisymmetric tornado with these velocities the total wind speed on the right (south) side of this tornado, $V + U$, must be at least 50 m s^{-1} (F2).

Tornado damage can be distinguished from downburst and microburst damage because tornadoes are characterized by convergence and large vorticity whereas downbursts are characterized by divergence and typically weak vorticity. Thus, a tornado damage pattern exhibits confluence and some sense of rotation, while downburst damage exhibits a diffluent pattern. When the tornado is weak and translating rapidly, the distinction is more difficult. Fujita (1978, 1981) and Fujita and Wakimoto (1981) give numerous examples of the damage produced by these phenomena.

In the absence of real-time measurements or motion pictures of a damaging wind storm, inferences about values of wind velocities, vorticity and divergence can sometimes be made from the damage pattern. For example, if there is a spatial pattern in the damage that suggests that in a limited area the damage was produced essentially simultaneously by nearly straight winds, then a gradient of the damage intensity (F-scales) normal to the wind direction implies shear vorticity.

Cyclonic shear vorticity was inferred along the northern edges of most of the microburst swaths on 6 August 1977. For example, the cyclonic shear was very large along the north side of downburst 9 of Fig. 1. Using the spacing between the F0 and F1 contours on the original detailed survey maps, the horizontal shear was estimated as 15 m s^{-1} over a distance of 250 m. This gives a rough estimate of the downburst-related horizontal shear vorticity, $\zeta \approx 6 \times 10^{-2}\ s^{-1}$.

Diffluence in the damage pattern normally implies divergence. Diffluence from a point (e.g., in microburst 11 of Fig. 1) indicates a short-lived outflow. If the downburst accompanying the outflow is translating, then the outflow damage pattern is fan-shaped rather than circular (Fig. 2). An elongated swath of downburst damage, such as downburst 9 of Fig. 1, indicates a sustained translating downburst. An estimate of the horizontal divergence associated with downburst 9 of Fig. 1, based upon rate of expansion of the F0 damage, is $1.5 \times 10^{-2}\ s^{-1}$.

A sufficient condition for confluence in the damage pattern to indicate convergence is for the pattern to culminate in a vortex, such as shown in Fig. 3. Based on the rapid confluence of streaklines of damage at this location, horizontal divergence is estimated as $-1.6 \times 10^{-1}\ s^{-1}$. Caution must be exercised regarding other confluent patterns. They sometimes represent *sequential* strong winds of differing directions, initially from the west-southwest and subsequently from the west-northwest. An example of this occurred near the "confluence" of microburst 7 and downburst 7 of Fig. 1, shown in Fig. 4.

Even without substantial evidence of vorticity and confluence patterns in the damage (i.e., when VU^{-1} is small), paths of vortices are generally unmistakably clear in corn fields and wheat fields. Their damage paths are distinguished from microbursts and down-

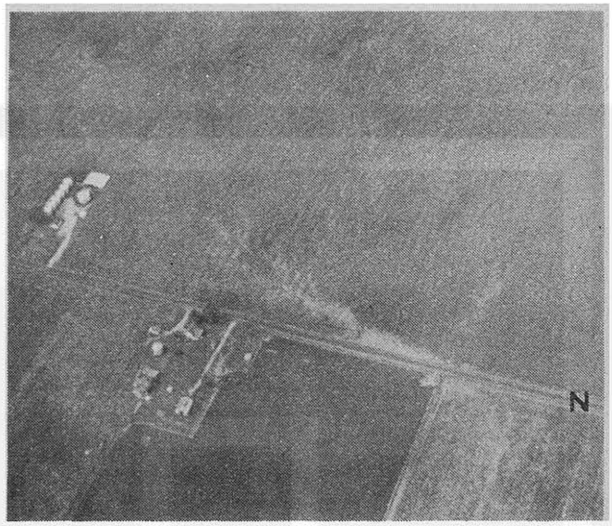

FIG. 3. Photograph of a spin-up mark associated with one of the multiple stray suction vortices in tornado 7, looking WSW. Diameter of the tornado's path of solid destruction is about 10 m and left–right width of the figure is about 550 m.

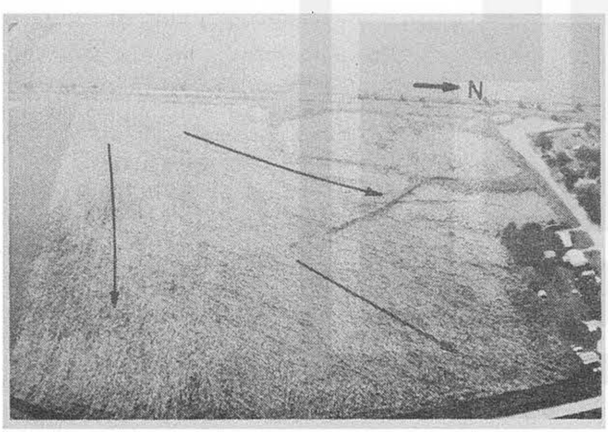

FIG. 2. Photograph of damage from microburst 11, looking west. Streamlines represent direction of corn fall. Left–right width of the photo represents about 400 m.

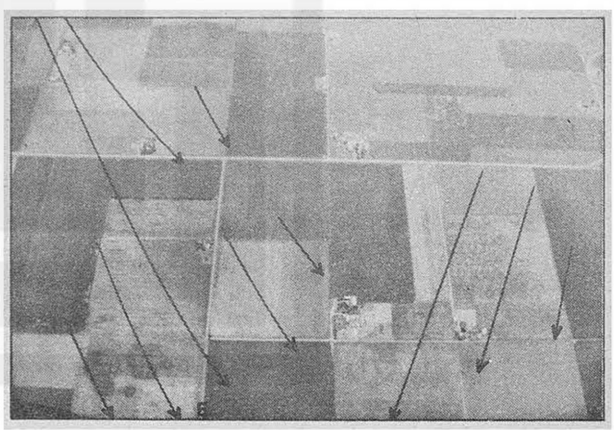

FIG. 4. Photograph of damage to corn near the junction of downburst 7 and microburst 7, looking west. Left–right width of the photo represents about 3.2 km.

bursts in several ways. The vortex path is usually sharply defined by a "line" of intense crop damage, and a sharp transition to much lesser damage on the periphery (Figs. 3 and 5). When viewed from the proper perspective at low sun angles, confluent or "herringbone-patterned" cropfall is easily detected, marking the vortex path (Fig. 5). Some tornadoes are also characterized by multiple swath marks (Fig. 6) and poorly defined looping marks.

Fig. 7 shows the path of the anticyclonic tornado (number 11 of Fig. 1) on 6 August 1977. The tornado was moving from south to north (bottom to top in Fig. 7) with looping marks on its right side, opposite those of a cyclonic tornado. The marks begin on the "weak-wind" side of the tornado path and are not fully closed loops, suggesting that the suction vortices did not make complete revolutions about the tornado, consistent with observations of a cyclonic tornado by Agee *et al.* (1975) and Forbes (1978). Ground-based proof of the anticyclonic rotation is shown in Fig. 8. Looking northward (top of photo) from a spot just west of the tornado center line, corn initially fell from the southwest and subsequently from the southeast as the tornado proceeded northward.

Though these techniques for classifying damage patterns are general guidelines, experience is invaluable for accurate and efficient assessment of the damage pattern. Also, it is very desirable to perform aerial surveys, ground surveys and resident interviews in regions of complicated damage, in order to obtain the best possible interpretation of the damage pattern. During the interviews, it is worthwhile to ascertain whether or not significant hail occurred with the strong winds. Towery *et al.* (1976) note that winds greatly increase the damage caused by hail. Similarly, the presence of large hail driven by winds of slightly less than damaging speed may nevertheless result in what appears to be wind damage. With this in mind, the authors asked residents whether hail occurred, and checked corn for bruising and shredding. It was concluded that hail was either non-existent or quite insignificant on 6 August 1977. Accordingly, streaks in the corn damage patterns shown in Fig. 4, very similar to that Towery and Morgan (1977) referred to as "hailstripes," can be caused by wind without hail being present (e.g., Figs. 2, 4).

FIG. 6. Photograph of suction swaths in tornado 10, looking north. The path of the anticyclonic tornado can be seen at lower right. Left–right width of the photo represents about 600 m.

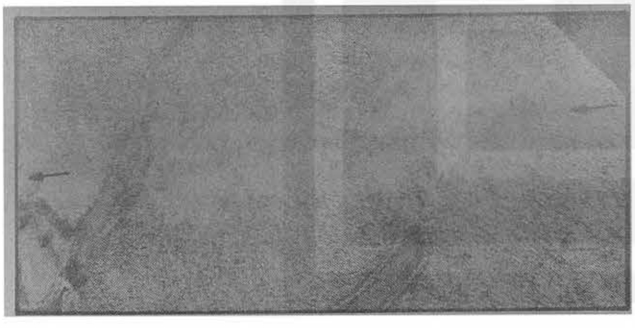

FIG. 5. Photograph of the path of tornado 17 through a corn field, looking SE. Left–right width of the photo represents about 200 m.

FIG. 7. Photograph of the path of the anticyclonic tornado 11, looking north. Arrows point to well-defined suction swath loop marks. Left–right width of the photo represents about 250 m.

FIG. 8. Pattern of corn fall in the anticyclonic tornado, looking north from a point just west of tornado center.

TABLE 1. FPP classifications* of the 18 Springfield-area tornadoes of 6 August 1977.

Name	F	P_L	P_W
1. Auburn	1	2	2
2. Waverly	0	0	3
3. Maxwell	0	0	0
4. Thayer	1	2	1
5. Loami Township	1	1	3
6. Divernon	1	2	2
7. South Fork	2	2	3
8. Twin	1	1	1
9. Glenwood Park	3	2	2
10. Brush Creek	1	2	2
11. Brush Creek anticyclonic	0	0	0
12. Ball School	0	0	1
13. Beamington	0	0	0
14. Pawnee	1	2	1
15. New City	1	1	1
16. Lake Kincaid	0	1	0
17. Breckenridge	1	1	1
18. Buckhart	1	2	3

* F-scale classification of tornado intensity and Pearson scales of path length (P_L) and path width (P_W) are defined by Fujita (1973).

3. Downbursts, microbursts and tornadoes on 6 August 1977 near Springfield, IL

Tornado paths and swaths of downburst and microburst wind damage were located during four days of aerial surveys, and documented by detailed mapping on topographic maps (scale 1:24 000) and by roughly 1600 color photographs. The authors subsequently interviewed residents on three days, obtaining information about the sequence of weather events during the storm. Downbursts 1 and 2 occurred beyond the west edge of the region shown in Fig. 1, and microburst 18 occurred beyond the east edge, as damage extended 14 km west and 29 km east of the region shown in Fig. 1. Overall, the swath of wind damage was over 106 km long and averaged 8–10 km in width, affecting portions of at least five counties. In some regions the swath was 13 km wide. With this windstorm, which occurred between 2100 and 2230 GMT, also came torrential rains which caused flash flooding.

Damage from the downbursts, microbursts and tornadoes was primarily to crops and trees. Downburst 9 caused minor damage to at least 10 structures, the worst of which are indicated by damage streaks in Fig. 1. Winds were so strong in this area that residents were sure they had been hit by a tornado. A Cessna 140 aircraft crashed in this downburst east of I-55, as noted on Fig. 1 [see Forbes and Wakimoto (1978) for additional details]. Only eight of the tornadoes (4, 6, 9, 10, 14, 15, 17, 18) caused damage to structures. Of these, number 9 was the most destructive. Most of the tornadoes were weak and short-lived. FPP classifications of the tornadoes are listed in Table 1.

Tornado 9 struck the Glenwood Park housing development east of Springfield, heavily damaging or demolishing 20 homes and causing lesser damages to at least 20 others. This tornado was classified as F3. Fig. 9 is a detailed mapping of the latter half of the path of this tornado, which displayed suction vortex swaths, loops in the debris patterns, and an abrupt left turn.

A phenomenon became apparent in association with this outbreak that had not been evident in the authors' prior surveys. Small pockets (with diameter of about 5–10 m) of isolated damage, much smaller than those of typical microbursts, were observed to the right (southeast) of the path of the tornado, at locations A and B of Fig. 9, where houses were damaged. The damage pattern at A resembled that of a tiny microburst with diameter of about 10 m, and has been termed a "blow-down spot." The divergent damage pattern at MB may have been this type of phenomenon. Blow-down spots were also observed to the right of tornadoes 1 and 8, with an example shown in Fig. 10. The cause of these blow-down spots is not known. However, it is not uncommon to observe downward motion in the outer portions of a tornado debris cloud. Golden and Purcell (1978) reported low-level downward motion on the right periphery of the Union City tornado. One of us (Forbes) has witnessed a blow-down spot-like phenomenon on the periphery of weak vortices in the University of Chicago laboratory model (see Fujita, 1977). These observations prompt the speculation that blow-down spots are the manifestation of a tornado-induced peripheral circulation.

Tornadoes 2, 7 and 8 appeared to contain a different type of suction vortex, defined as a "stray vortex" by Fujita (1976a). These vortices occur in very close proximity to one another but show little tendency to revolve about each other, as if the parent tornado circulation is very weak and the stray vortex circulation is extremely limited in radial extent. The path of one of the stray vortices of tornado 7 is shown

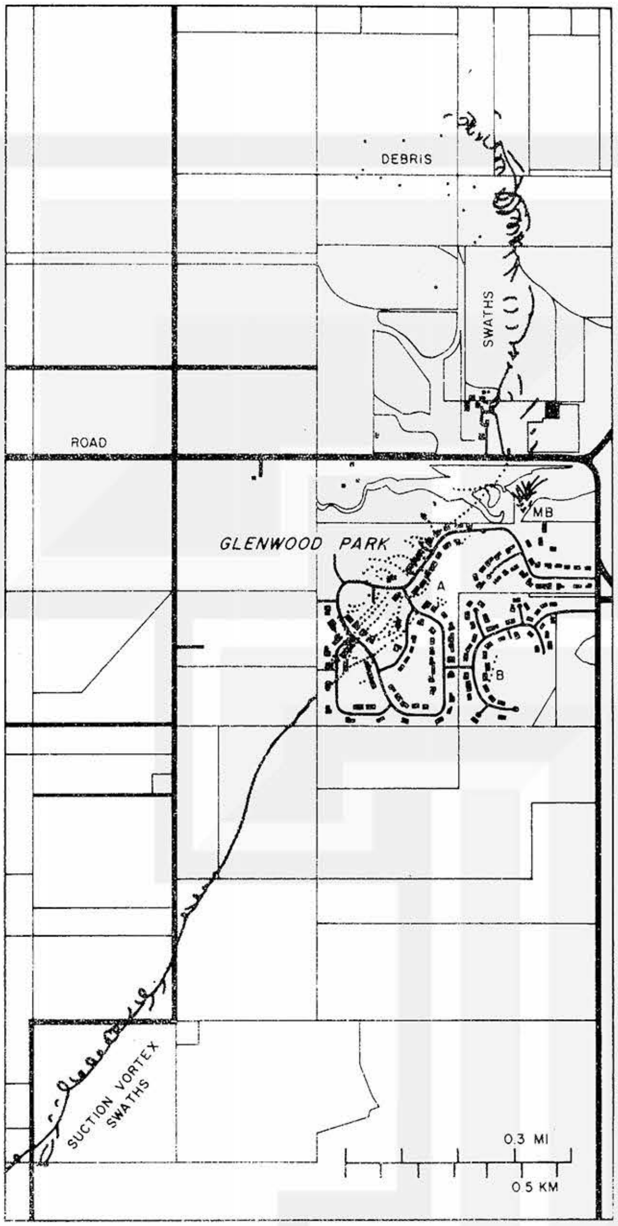

FIG. 9. Path of the latter half of tornado 9, as it passed through Glenwood Park. Heavy lines represent roads and thin lines represent edges of fields. Dots and dotted lines denote debris and debris swaths.

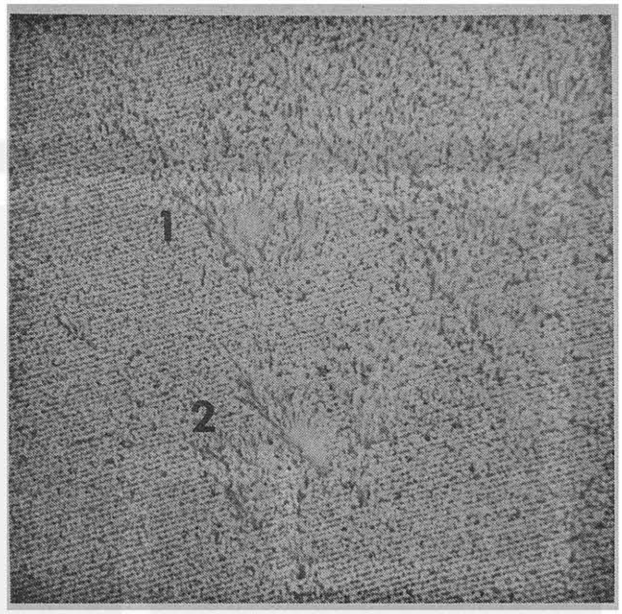

FIG. 10. Photograph of blow-down spots on the southeast side of tornado 1. Diameter of spots is 5–10 m.

in Fig. 3. Davies-Jones *et al.* (1978) report haphazardly-distributed swirls that may have had a similar origin within the damage pattern of the Union City, Oklahoma tornado.

4. Synoptic and mesoscale aspects of the 6 August 1977 storm

The Springfield-area storm was not associated with an extensive, rapidly-moving squall line. Instead, the windstorm was associated with a mesoscale echo configuration referred to as a bow echo (Fujita, 1978, 1981). The bow echo occurred just south of a slow-moving (almost stationary) cold front. The storm developed in the vicinity of the intersection of a moisture front and thermal boundary [of the type described by Maddox *et al.* (1980)], which resulted from thunderstorms during the previous night. Temperatures and dewpoints in the warm sector were about 32 and 22°C, respectively. The downburst thunderstorms were triggered by the approach of a weak 500 mb trough. Additional details of the synoptic situation are given by Forbes and Wakimoto (1978), and general synoptic-scale conditions favorable for downburst thunderstorms are discussed by Forbes *et al.* (1980).

Fujita (1978) observed that the potential downburst region can be identified in radar and satellite imagery: at the leading edge of a bow echo on radar, and just ahead of a warm spot in a large anvil area in satellite imagery. Downburst-producing thunderstorms are sometimes embedded in convective systems which resemble mesoscale convective complexes (Maddox, 1980). Fig. 11 shows infrared imagery of this type associated with the downburst thunderstorms at 2100 and 2200 GMT (1500 and 1600 CST) on 6 August 1977, with radar echoes superimposed.

Fig. 12 shows the evolution of the radar echo pattern between 2127 and 2222 GMT. Most of the downbursts and tornadoes occurred during this time period, while the echo shape evolved from an arc or bow into a comma. The comma stage generally signals the imminent cessation of downburst activity. Dots on the figure indicate the best estimates of the locations of the downbursts and tornadoes relative to

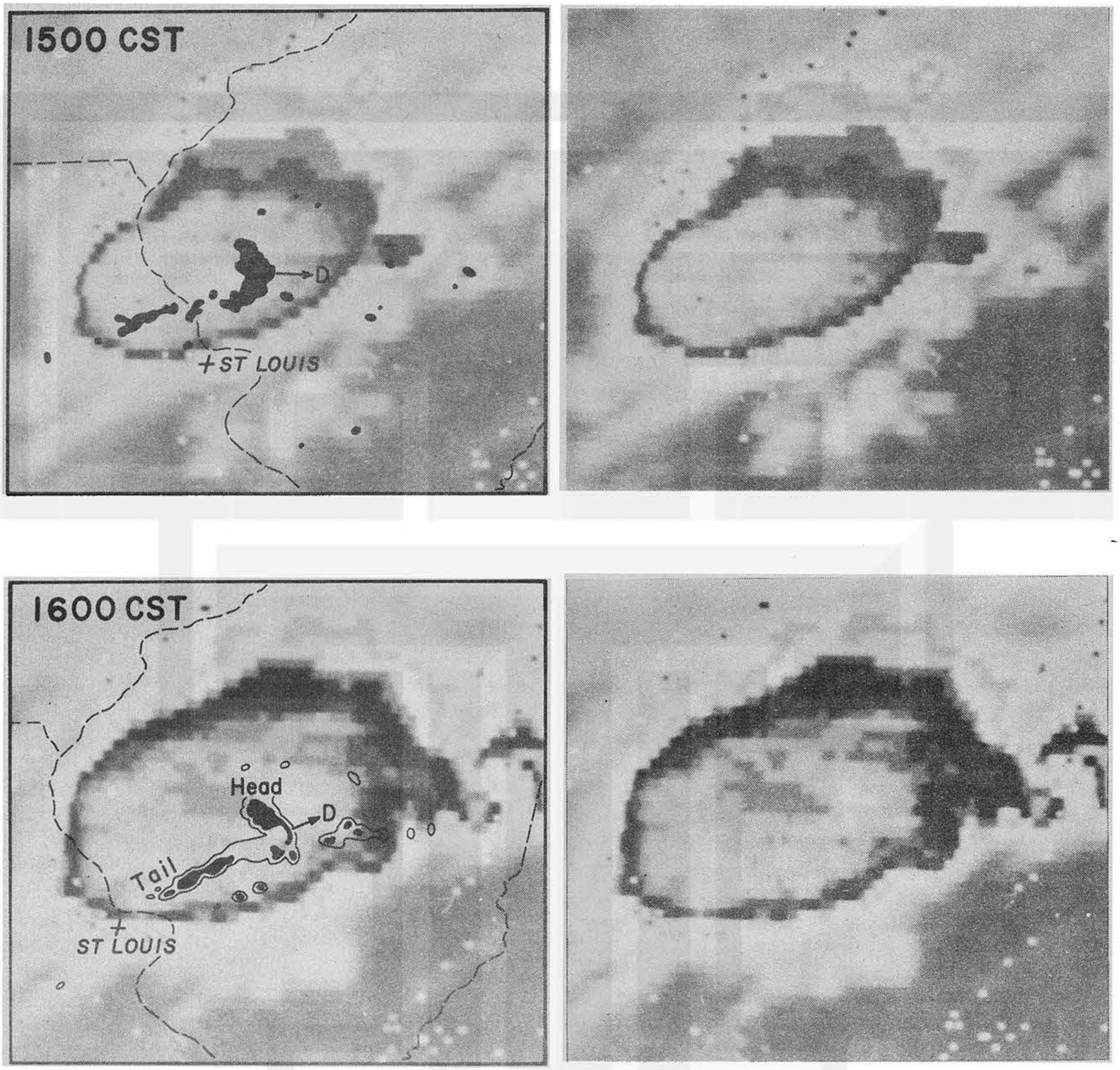

FIG. 11. Infrared satellite imagery (NESS enhancement curve MB) associated with the storm of 6 August 1977, at 2100 and 2200 GMT (1500 and 1600 CST) with radar imagery superimposed. Warm spots appear as gray areas surrounded by white. D denotes the axis of the downburst activity.

the echoes. It was not possible to pinpoint definitely the time of occurrence of each of the downbursts and tornadoes using standard survey techniques, such as clock stoppage, since only a few of the tornadoes were witnessed and the downbursts and tornadoes all occurred in close proximity. However, a few residents were able to pinpoint times of downburst and tornado occurrence, and each of the witnessed tornadoes occurred just prior to the onset of heavy rain and wind. Sometimes it was raining lightly as the tornado passed.

At least nine of the tornadoes (1, 4, 6, 8, 10, 11, 14, 15, 16) appeared to occur along the tail of the bow echo (just south of the surge region), near the southern dots of Fig. 12. An eyewitness to tornado 4 noted at the time of the tornado there was a rain shaft to the west and that it became windy after the tornado passed. Other residents in the vicinity of these tornadoes did not witness the vortices, but indicated that the winds were strong and gusty, though not strong enough to cause substantial damage. On the basis of the damage survey and eyewitness observations, it seems likely that these tornadoes occurred along a gust front associated with the tail of the bow echo.

Many of the other tornadoes appeared to occur

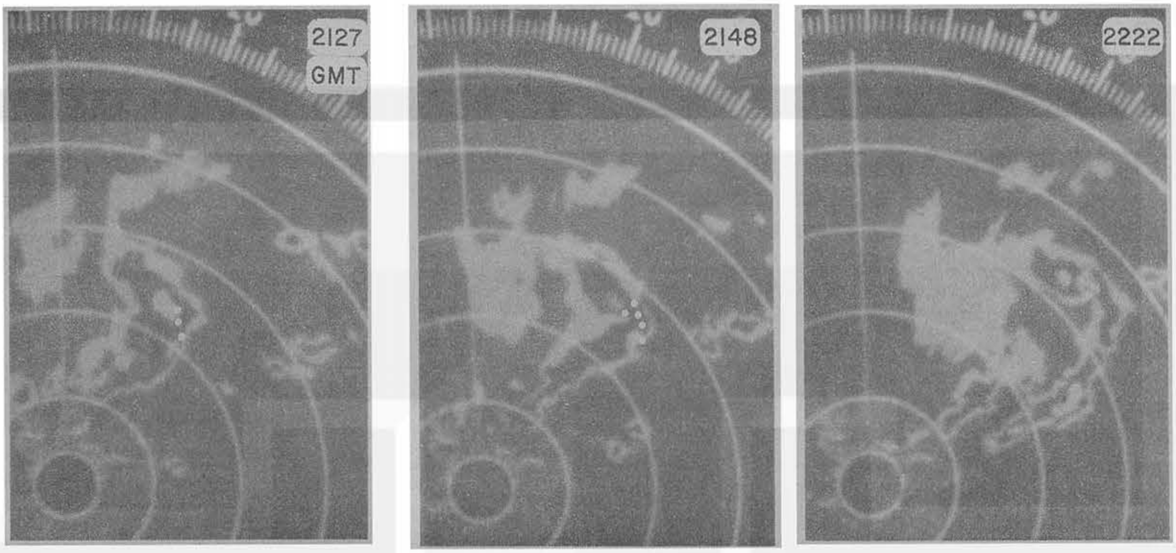

FIG. 12. PPI radar displays from the St. Louis radar at 2127, 2148 and 2222 GMT. Range marks are at 25 n mi (46 km) intervals. Innermost light shading is very strong echo, video integrator processor (VIP) level 4; surrounded by black, strong echo, VIP 3; and outer light, moderate echo, VIP 2. Dots indicate locations of downbursts and tornadoes. Elevation angle is near zero.

along the south side of the head (north portion) of the bow or comma echo configuration. Because the echo pattern was rotating slowly about an axis in the vicinity of the comma head, there may have been a mesocyclone present there. Hence, some of the downbursts, microbursts and tornadoes may have been associated with a mesocyclone.

5. Generation of tornadoes and other eddies

Vorticity can be generated through a number of processes. The change of magnitude of the vertical component of vorticity ζ of an element of fluid is

$$\frac{d(\zeta+f)}{dt} = \underbrace{-(\zeta+f)\left(\frac{\partial u}{\partial x}+\frac{\partial v}{\partial y}\right)}_{A} + \underbrace{\frac{\partial \alpha}{\partial y}\frac{\partial p}{\partial x} - \frac{\partial \alpha}{\partial x}\frac{\partial p}{\partial y}}_{B}$$

$$+ \underbrace{\frac{\partial w}{\partial y}\frac{\partial u}{\partial z} - \frac{\partial w}{\partial x}\frac{\partial v}{\partial z}}_{C} + \underbrace{\alpha\left(\frac{\partial F_y}{\partial x} - \frac{\partial F_x}{\partial y}\right)}_{D}, \quad (1)$$

where f is the Coriolis parameter; u, v and w are the components of velocity in the x, y and z directions, respectively; α is the specific volume; p is the pressure; and F_x and F_y are the components of the frictional force in the x and y directions. Term A is commonly referred to as the stretching term, term B as the baroclinic (solenoid) term, and term C as the tilting term. Term D represents viscous effects, and for a fluid with constant kinematic viscosity (ν), can be written $\nu\nabla^2\zeta$. Thus, under conditions of uniform viscosity, term D represents diffusion of vorticity.

Tornadogenesis is generally explained through terms A and B, representing stretching and tilting processes. Quantitative studies by Lemon and Doswell (1979) using Doppler radar data[1] indicate that large mesocyclone-related tornadoes occur at the downdraft–updraft interface where the tilting term is most significant in mid-troposphere. Stretching is a close rival, especially at low levels. Brandes (1981) indicates that at low levels the stretching term is most significant. Lemon and Doswell also indicated that the solenoid term (C) may contribute to tornadogenesis. Maxworthy (1973) proposed that tilting of vortex tubes associated with boundary layer vertical wind shear is the mechanism for tornadogenesis.

From only damage pattern information, it is not possible to state definitely which of the vorticity generating mechanisms was most significant for tornadogenesis on 6 August 1977. Some order of magnitude estimates of the values of some of the terms in (1) can be obtained, however. A representative value of downburst-related vorticity, 6×10^{-2} s^{-1}, and mean horizontal divergence associated with genesis of a stray suction vortex within tornado 7, -1.6×10^{-1} s^{-1}, were calculated in Section 2. Insertion of these values into (1) yields a vorticity generation rate of about 10^{-2} s^{-2} due to stretching.

Integrating the stretching term of (1) with respect to time yields the spin-up time Δt of a vortex (ignoring the Coriolis parameter, which is negligibly small on this scale:

$$\Delta t = -\frac{1}{\mathrm{DIV}} \ln\left(\frac{\zeta_{\mathrm{vortex}}}{\zeta}\right), \quad (2)$$

[1] A number of researchers have used Doppler radar data to evaluate the contributions of the terms of (1) to mesocyclogenesis. Only tornadogenesis studies have been cited here.

where $\overline{\text{DIV}}$ is the mean horizontal divergence during the period Δt, ζ is the initial vorticity, and ζ_{vortex} is the vorticity of the mature vortex. Based upon an estimate of the damaging wind speeds in Fig. 3 of 40 m s^{-1}, and a translation of 20 m s^{-1}, the tangential velocity of the suction vortex was $\sim$20 m s^{-1}. (Here the speed of revolution of this stray suction vortex about the tornado was negligible, as discussed in Section 3.) Assuming solid rotation about the vortex of radius $\sim$ 5 m, the vortex had vorticity $\zeta_{\text{vortex}} \approx 8$ s^{-1}. Using this with the above values of initial shear vorticity and mean divergence yields a spin-up time of the vortex from (2) of about 30 s, which is consistent with a subjective estimate of between 8 and 50 s, based upon inspection of Fig. 3. Hence, stretching of downburst- or microburst-related vorticity appears to be a possible mechanism for generation of vortices and tornadoes.

Values of the components of the tilting term (C) of (1) are most difficult to estimate. Damaging (20 m s^{-1}) winds at height of 2 m suggest extreme boundary layer vertical wind shear ($\partial u/\partial z \approx 10$ s^{-1}). Fujita (1980) has indicated that downward vertical velocities exceed 5 m s^{-1} in microbursts. Horizontal shears of vertical velocity along the edge of the downburst or microburst may be $\sim 5 \times 10^{-3}$ s^{-1} [based upon Figs. 9 and 10 of Fujita and Caracena (1977) and Fig. 29 of Fujita (1981)] to $\sim 2 \times 10^{-2}$ s^{-1} [based upon Fig. 8 in Fujita (1980)]. Hence, the magnitude of the tilting term in (1) is estimated as $\sim 5 \times 10^{-2}$ to 2×10^{-1} s^{-2}. If the magnitude of the tilting term is assumed constant with time, integration of (1) yields a spin-up time for the vortex in Fig. 3 of $\sim$40–160 s, which also seems reasonable. Thus, both stretching and tilting of boundary-layer vorticity appear to be possible mechanisms of downburst- and microburst-related vortex formation.

In the general formulation in (1) the viscosity may be assumed variable, and term D can explain the generation of vertical components of vorticity in the vicinity of topographic or artificial obstacles in the flow. The vortex sheet generated in this manner can become unstable and roll up into eddies in the wake of the obstacle. Examples of this phenomenon on the mesoscale include von Kármán vortex patterns in the field of stratocumuli in the wake of islands (Hubert and Krueger, 1962). Lemon (1976) has proposed that mesoscale vortices in the wake of a thunderstorm are generated in a similar manner.

Mechanical eddies produced by interaction of the flow with obstacles also occur on the microscale. Barcilon and Drazin (1972) report that dust devils can form through stretching of vertical vortex tubes which arise owing to Kelvin-Helmholtz instability within a vertical sheet of horizontal shear vorticity. The horizontal shear vorticity for the dust devil often arises owing to obstacles in the flow (Williams, 1948) or small-scale terrain features (Sinclair, 1969; Ingram, 1973; Idso, 1974).

Shear-induced swirls of diameter 5–10 m were observed in the damage patterns of 6 August 1977 in the wake of rows of trees, in von Kármán-like patterns. These swirls were located in the zone of horizontal wind shear downstream of the edge of the row of trees, as in Fig. 13.

Fig. 14 provides an overview of the same region, just east of Interstate 55 (see Fig. 1). Winds from microburst 18 interacted with the north end of the row of trees near A, producing the von Kármán-like pattern of Fig. 13. Winds from microburst 10 downed corn on the south (left) portion of the photograph. These winds interacted with the south edge of the row of trees near C. Some spotty damage east of D indicates that some wind penetrated through an open-

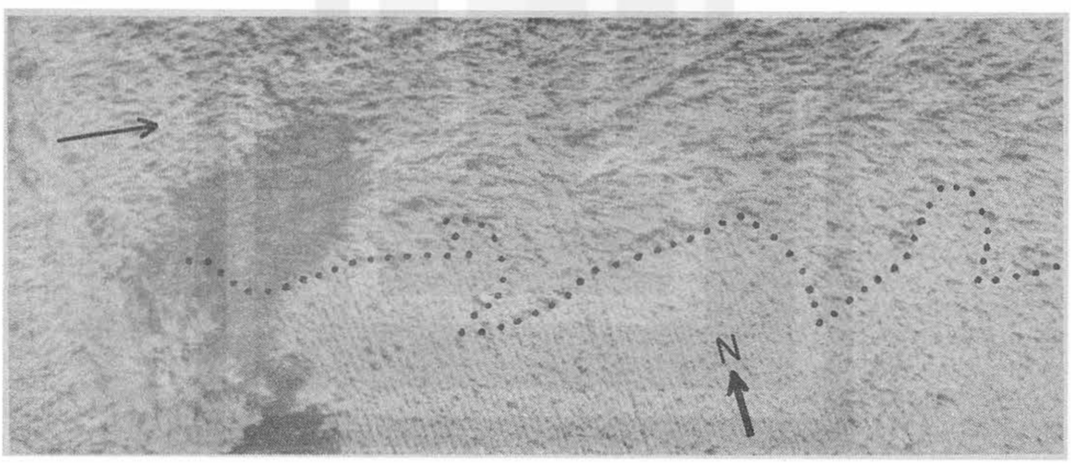

FIG. 13. Photograph of von Kármán-like patterns in corn damage associated with microburst 18, downstream of the edge of a row of trees, looking NNE. Corn damage from west-northwest winds is extensive at the top of the photo and negligible downwind of the trees near the bottom of the photo. Left–right width of the photo represents about 150 m. Edge of tree row is at A of Fig. 14.

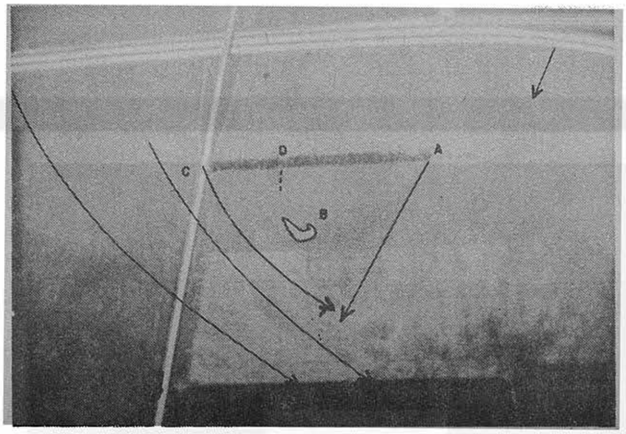

FIG. 14. Photograph of the junction of microbursts 10 and 18, looking west. A swirl formed at B along the left edge of microburst 18, whose shear may have been increased due to interaction with the row of trees at C. Left–right width of the row of trees (A–C) represents about 330 m.

ing in the row of trees at that location. A marked swirl occurred at B, shown in close-up in Fig. 15. Figs. 14 and 15 suggest that the swirl at B was due to a short-lived vortex which developed in association with 1) horizontal shear along the north side of microburst 10 and 2) enhanced horizontal shear resulting from interaction of the southwesterly flow with the tree row near C. The sign of the shear vorticity from each of these contributions is positive, and the swirl at B appears to be cyclonic.

An inspection of Fig. 1 suggests that tornadoes may form from the shears on the periphery of microbursts, as suggested above, even in the absence of orographic or other obstacles (e.g., rows of trees). Tornadoes 2, 3, 5, 7, 9, 12, 13 and 18 all formed just downstream and on the cyclonic shear side of microbursts. The Kelvin-Helmholtz instability discussed by Barcilon and Drazin (1972) may be a mechanism of formation of these tornadoes.

FIG. 15. Closeup photograph of the swirl in Fig. 14, looking west. Swirl has diameter of ~35 m.

These microburst-related tornadoes may also have been in the immediate vicinity of the mesocyclone accompanying the head portion of the comma echo discussed in Section 4. Nevertheless, the close spatial relationship between the microbursts and tornadoes in Fig. 1 suggests that the vorticity source for these tornadoes was boundary-layer horizontal or vertical shear accompanying the microbursts. The downdrafts of these microbursts may have been acting as agents for the transport (downward flux) of horizontal momentum from the mesocyclone aloft into the boundary layer. Because of the localized nature of the microbursts, large horizontal shears would develop on the periphery of these zones of momentum flux, providing a source of tornadic vorticity. This downward flux is consistent with reports by Lemon *et al.* (1977) that the Doppler mesocyclone signature descends toward the surface in association with tornadogenesis.

Fujita (1979) indicates that two tornadoes on 25 June 1978 formed on the leading edge of a downburst confirmed by Doppler radar. Although the damage suggested that there was downburst-related cyclonic shear in the vicinity of the tornado, Doppler radar showed the tornado *directly ahead* of the downburst, rather than on its left flank. This suggests that vortex development associated with shear instability may also occur along the leading edge of downbursts. Spin-up is expected to be rapid owing to large values of convergence at the downburst-environment interface.

It can be seen from Fig. 1, as discussed in Section 4, that tornadoes 1, 4, 6, 8, 10, 11, 14, 15, 16 and 17 did not have damaging microbursts near their point of touchdown. Most of these tornadoes appeared to form along the gust front (though origin is uncertain for 17). Other researchers (Burgess and Donaldson, 1979; Wilson *et al.*, 1980) have reported the development of tornadoes along the gust front and suggest that they develop as a result of shearing instability of the type discussed by Barcilon and Drazin (1972). Similar developments of tornadoes have been reported from shearing instabilities associated with cold fronts (Testud *et al.*, 1980; Wilson *et al.*, 1980; Carbone and Serafin, 1980; Carbone, 1982) and within mesocyclones (Brandes, 1977; 1978). Golden (1974) and Barnes (1978) indicate that waterspouts and mesocyclones, respectively, may also develop as a result of this type of shearing instability.

6. Classification of tornadoes

The *Glossary of Meteorology* (Huschke, 1959) defines the tornado as "a violently rotating column of air, pendant from a cumulonimbus cloud, and nearly always observable as a funnel cloud or tuba." The general term for a small-scale rotating column of air is the "whirlwind," with dust whirl, dust devil, waterspout and tornado listed as specific forms. These guidelines are rather vague, and place high priority on eyewitness observations of the tornado and its parent cloud. The meteorologist surveying the damage from an unwitnessed vortex or other windstorm must make a classification decision, nevertheless. We took the liberty of classifying all non-wake vortices on 6 August 1977 as tornadoes because they produced damage and because they were associated with a severe thunderstorm system.

It is not uncommon for documented "tornadoes" to appear primarily in the form of a low-level dust and debris cloud, occasionally without any visible condensation funnel (e.g., Golden and Purcell, 1977; Lemon *et al.*, 1980). Fig. 16 shows three vortices, which Burgess and Donaldson (1979) referred to as gust front tornadoes, that formed along the leading edge of the outflow from a nearby thunderstorm. From eyewitness observations, it seems that tornadoes 4 and 18 on 6 August 1977 resembled these gust front tornadoes, and did not possess funnel clouds. There is, of course, a possibility that an unnoticed funnel did exist near cloud base. Funnel clouds were observed with tornadoes 2, 9 and 17. The other 13 tornadoes were not observed.

It is clear, therefore, that at least two of the 6 August 1977 "tornadoes" may not have possessed funnel clouds. Also, it is possible that not all 18 tornadoes were directly pendant from a cumulonimbus, and some were not particularly violent. In many cases, the wind speeds in the tornadoes were probably only 15–20 m s^{-1} greater than the microburst and downburst winds in the vicinity.

Some scientists (e.g., Ingram, 1973) have resisted classifying damaging vortices as tornadoes unless all *Glossary* criteria were met. Other documented "tornadoes" in the literature fail to meet requirements in the *Glossary* definition. Bates (1968), Barnum *et al.* (1970), Moller (1978) and Burgess and Davies-Jones (1979) cite tornadoes which developed pendant from growing cumuli and congestus in flanking lines associated with nearby cumulonimbi. Bluestein (1980) observed funnel clouds and eddies associated with flanking lines and along gust fronts.

Under ideal circumstances the classification of atmospheric vortices is straightforward. Vortices with wind speeds exceeding 70 m s^{-1} or producing F3 tornado damage (Fujita, 1973), connected by a funnel cloud to a severe thunderstorm, are unquestionably tornadoes by any definition. Vortices accompanying cumuli off the Florida Keys are unquestionably waterspouts. Vortices triggered by a moving vehicle over a flat desert on a calm day under a cloudless sky are unquestionably dust devils. A scan of the literature indicates that virtually any other combination of cloud, nearby water body, presence or absence of funnel cloud, and short-lived vortex with winds near 25 m s^{-1} results in confusion.

Table 2 lists "borderline" vortical phenomena reported in the literature. The list is not intended to be comprehensive, preferentially citing articles containing numerous cases or extensive bibliography, or those readily available. Because the synoptic conditions under which they form differ from their mid-

FIG. 16. Photograph of three vortices which formed along the leading edge of the outflow from a nearby thunderstorm on 21 August 1979 near Pawnee, OK. Courtesy of G. Moore, D. Perry and B. F. Smull.

TABLE 2. Examples of atmospheric vortices which challenge *Glossary of Meteorology* definitions.

Phenomena	References
Tornadoes from developing thunderstorms or flanking cumuli*	Barnum *et al.* (1970) Burgess and Donaldson (1979)
Gust front, downburst, and other shear zone tornadoes*	Wilson *et al.* (1980)
Tornadic waterspouts	Dinwiddie (1959) Golden (1971)
Dust devils over water	Idso (1975a)
Whirlwind at sea breeze front	Meaden (1981)
Dust devils along sea breeze front	Simpson (1969)
Desert whirlwinds	Idso (1974, 1975b)
Eddy tornadoes	Ingram (1973)
Mountainadoes	Bergen (1976)
Cold air funnels	Cooley (1978)
Steam devils over lake	Lyons and Pease (1972)
Fire whirlwinds	Graham (1955) Church *et al.* (1981)
Volcano whirlwinds	Thorarinsson and Vonnegut (1964)

* Refer to text in Sections 1, 5 and 6 for additional references.

western counterpart (Novlan and Gray, 1974), hurricane-induced tornadoes could be added to the list.

Most of the phenomena listed in Table 2 are easily understood from their descriptive names. Desert whirlwinds, eddy tornadoes and mountainadoes merit further explanation. Ingram (1973) believes that many Arizona tornadoes are really eddies induced by local topographic obstacles within a field of strong straight-line winds. The source of the strong straight-line wind is often the outflow from a nearby thunderstorm. Mountainadoes (Bergen, 1976) occur during winter downslope windstorms in the lee of topographic barriers. Idso's (1974, 1975b) desert whirlwinds appear to be of two types: the eddy tornado type and a second type which develops along or just ahead of the frontal boundary of the dust storm or haboob (i.e., just ahead of, rather than within, the strong straight-line winds). Warn (1952) describes dust devils and gives a remarkable description of whirlwinds along strong cold fronts, along the leading edge of thunderstorm outflow, and in association with thunderstorm updrafts.

In pondering the table of "borderline" atmospheric vortices, some basic principles ultimately assert themselves. (i) Tornadoes should be naturally-occurring convective vortices rather than mechanically or artificially induced vortices and should be capable of producing damage. (ii) Some distinction should be maintained between tornadoes accompanying thunderstorms and other damaging vortices, on the basis of both tradition and meteorological considerations. (iii) In keeping with the dominant phrase in Huschke's definition, "violently rotating column of air," all damaging vortices deserve tornadic rank. Accordingly, we propose the following pragmatic definitions: A vortex is classified as a *tornado* 1) if it produces at least F0 damage or exhibits wind speeds capable of producing such damage and 2) if it forms in association with the wind field of a thunderstorm or its accompanying mesoscale features, such as the gust front and flanking line. Damaging vortices not associated with thunderstorms are referred to as *tornadic vortices of a particular type*, such as tornadic waterspout. Non-damaging vortices retain their present *Glossary* definitions.

Invoking these pragmatic definitions clarifies the classification of the "borderline" vortices of Table 2. Mechanically-induced vortices in the lee of shelterbelts and topographic features are eliminated from consideration as tornadoes. Thus, mountainadoes (also eliminated because they are associated with winter downslope windstorms rather than thunderstorms) and most dust devils are eliminated. Dust devils or eddy tornadoes associated with haboobs, triggered by thunderstorm outflow (Idso *et al.*, 1972), are considered tornadoes if they produce damage.

Steam devils, fire whirlwinds and volcano whirlwinds are tornadic vortices under normal circumstances, when they are not associated with thunderstorms [although Fujita (1973) reports that fire tornadoes developed from cumulonimbus clouds during the 1923 Tokyo fire]. Cold air funnels can be tornadic vortices or tornadoes, as they sometimes occur in association with thunderstorms, but are normally non-tornadic because they do not touch ground or produce damage.

Under normal circumstances the other vortices of Table 2 are considered tornadoes if they produce damage. Thus, thunderstorm-related waterspouts moving inland, tornadoes from flanking cumuli and along the gust front, and tornadoes associated with downbursts and microbursts are included as tornadoes. Inclusion of these phenomena as tornadoes and tornadic vortices in climatological data bases should allow for an accurate assessment of the hazard due to atmospheric vortices.

Suction vortices embedded within a damaging tornado are not classified as separate tornadoes, though it would be useful if their presence were noted in *Storm Data*. Stray suction vortices, associated with a weak tornado circulation, are somewhat problematic in that the swaths may be relatively widely separated. Here the distinction between multiple suction vortices and separate tornadoes is somewhat arbitrary, but stray vortices and their swaths separated by less than 1 km should probably be considered multiple vortices of a weak parent tornadic circulation.

Classification of "eddy tornadoes" and downburst- and microburst-related vortices as tornadoes may increase tornado frequency statistics somewhat in regions where such phenomena are not now classified as tornadoes. Frequency alone, however, is not a good indicator of tornado hazard, since a fraction of all tornadoes—the strong ones, which also are generally long-lived—produce most of the yearly damage and fatalities (Kelly *et al.*, 1978). Additionally, some tornadoes inevitably are unreported and some wind damage is incorrectly classified as tornadic. There are also cases in *Storm Data* where multiple vortices within a tornado have been reported as several tornadoes. A more realistic assessment of tornado hazard includes information on *area affected*, and intensity, in addition to frequency (Abbey and Fujita, 1975). Tornado-hazard assessments of the latter type should not be greatly affected if a few additional damage occurrences in a region are now classified as tornadic.

7. Conclusions and discussion

A detailed survey of the damaging windstorm near Springfield, Illinois on 6 August 1977 revealed the occurrence of 10 downbursts, 19 microbursts, 17 cyclonic tornadoes, and one anticyclonic tornado. The 18 tornadoes occurred within a 20 km × 40 km area in a 45 min period. The tornadoes were associated with a bow echo configuration on radar; no hook echoes were observed. Many of the tornadoes appeared to develop in conjunction with wind shears associated with the gust front and with microbursts.

Many of the tornadoes did not conform to the definition listed in the *Glossary of Meteorology*, as many of the tornadoes were 1) weak and short-lived, 2) without funnel cloud, and 3) not necessarily pendant from a cumulonimbus. More pragmatic definitions are suggested in Section 6, and adopted in this case study. A vortex is classified as a *tornado* (i) if it produces at least F0 damage or exhibits wind speeds capable of producing such damage and (ii) if it forms in association with the wind field of a thunderstorm or its accompanying mesoscale features, such as the gust front and flanking line. Damaging vortices not associated with thunderstorms are considered *tornadic vortices of a particular type.*

The case study presented in this paper is significant in that it calls attention to a severe weather event that was rather different from most others cited in the literature. Whereas supercell thunderstorms producing families of major tornadoes have been the subject of concentrated research, less research has been done on the origin of weak tornadoes. Nevertheless, a number of such studies have been cited, and this partial survey reveals that the origins are varied.

As future meteorological service programs such as NEXRAD and PROFS evolve from the planning to operational stages, it would be useful if some feedback could be obtained from a national severe weather reporting system. Whereas research has provided a basis for a successful program of detection of mesocyclones and major tornadoes, on a national basis relatively little is known regarding even the frequency of occurrence of various other severe weather subtypes. It would be useful if comments could be inserted in *Storm Data*, for example, that would indicate the occurrence of severe weather in these atypical contexts. For example, it would be useful to know whether or not a hook echo or bow echo was observed and whether the tornado or tornadic vortex could be sub-classified as one of the types in Table 2. Such information would provide valuable feedback to the research community, indicating situations urgently in need of study. Efforts should continue which are devoted to broadening the research base regarding various severe weather situations.

Acknowledgments. The authors are grateful to scores of cooperative residents who gave eyewitness accounts of the storm. The authors benefitted from discussions with Prof. T. Fujita, who participated in the analysis of this case (Fujita, 1978) and prepared the final drafting of Fig. 1. The authors wish to thank Gene Moore, Dale Perry and Bradley F. Smull for the use of their photograph (Fig. 16); and Don Burgess for assistance in obtaining the photograph and for valuable comments about our case study. Bradley F. Smull, Leslie R. Lemon, and an anonymous reviewer all made many helpful comments on the manuscript. The Illinois Department of Law Enforcement, Support Services Division, provided aerial survey photographs which were useful in the preparation of Fig. 9. The research was sponsored by the Nuclear Regulatory Commission under Contract 04-74-239, by the National Oceanic and Atmospheric Administration under Grant NA80 AA-D-00001, and by the National Aeronautics and Space Administration under Grant NGR 14-001-008.

REFERENCES

Abbey, R. F., Jr., and T. T. Fujita, 1975: Use of tornado path lengths and gradations of damage to assess tornado intensity probabilities. *Preprints 9th Conf. Severe Local Storms*, Norman, Amer. Meteor. Soc., 286–293.

Agee, E. M., C. Church, C. Morris and J. T. Snow, 1975: Some synoptic aspects and dynamic features of vortices associated with the tornado outbreak of 3 April 1974. *Mon. Wea. Rev.*, **103**, 318–333.

Barcilon, A. I., and P. G. Drazin, 1972: Dust devil formation. *Geophys. Fluid Dyn.*, **4**, 147–158.

Barnes, S. L., 1978: Oklahoma thunderstorms on 29-30 April 1970. Part II: Radar-observed merger of twin hook echoes. *Mon. Wea. Rev.*, **106**, 685–696.

Barnum, D. C., D. E. Martin, A. T. Safford and J. L. Vogel, 1970: F. C. Bates' conceptual thoughts on severe thunderstorms. *Bull. Amer. Meteor. Soc.*, **51**, 481–488.

Bates, F. C., 1968: A theory and model of the tornado. *Proc. Int. Conf. Cloud Physics*, Toronto, Amer. Meteor. Soc., 559–563.

Bergen, W. R., 1976: Mountainadoes: a significant contribution to mountain windstorm damage? *Weatherwise*, **29**, 64–69.

Bluestein, H. B., 1980: The University of Oklahoma severe storms intercept project—1979. *Bull. Amer. Meteor. Soc.*, **61**, 560–567.

Brandes, E. A., 1977: Gust front evolution and tornadogenesis as viewed by Doppler radar. *J. Appl. Meteor.*, **16**, 333–338.

——, 1978: Mesocyclone evolution and tornadogenesis: Some observations. *Mon. Wea. Rev.*, **106**, 995–1011.

——, 1981: Finestructure of the Del City-Edmond tornadic mesocirculation. *Mon. Wea. Rev.*, **109**, 635–647.

Burgess, D. W., and R. P. Davies-Jones, 1979: Unusual tornadic storms in eastern Oklahoma on 5 December 1975. *Mon. Wea. Rev.*, **107**, 451–457.

——, and D. R. Devore, 1979: Doppler radar utility in severe weather warnings. *Preprints, 11th Conf. Severe Local Storms*, Kansas City, Amer. Meteor. Soc., 577–579.

——, and R. L. Donaldson, Jr., 1979: Contrasting tornadic storm types. *Preprints 11th Conf. Severe Local Storms*, Kansas City, Amer. Meteor. Soc., 189–192.

——, R. A. Brown, L. R. Lemon and C. R. Safford, 1977: Evolution of a tornadic thunderstorm. *Preprints 10th Conf. Severe Local Storms*, Omaha, Amer. Meteor. Soc., 84–89.

Carbone, R. E., 1982: A severe frontal rainband. Part I: Stormwide hydrodynamic structure. *J. Atmos. Sci.*, **39**, 258–279.

——, and R. Serafin, 1980: A severe winter squal line, Part II: Kinematic structure deduced from triple Doppler radar observations. *Preprints 19th Conf. Radar Meteorology*, Miami, Amer. Meteor. Soc., 9–16.

Church, C. R., J. T. Snow and J. Dessens, 1981: Intense atmospheric vortices associated with a 1000 MW fire. *Bull. Amer. Meteor. Soc.*, **61**, 682–694.

Cooley, J. R., 1978: Cold air funnel clouds. *Mon. Wea. Rev.*, **106**, 1368–1372.

Davies-Jones, R. P., D. W. Burgess, L. R. Lemon and D. Purcell, 1978: Interpretation of surface marks and debris patterns from the 24 May 1973 Union City, Oklahoma tornado. *Mon. Wea. Rev.*, **106**, 12–21.

Dinwiddie, F. B., 1959: Waterspout-tornado structure and behavior at Nags Head, NC, August 12, 1952. *Mon. Wea. Rev.*, **87**, 239–250.

Forbes, G. S., 1978: Three scales of motions associated with tornadoes. U.S. Nuclear Reg. Comm., Contract Rep. NUREG/CR-0363, 359 pp. [NTIS PB-288291].

——, and R. M. Wakimoto, 1978: Downbursts and tornadoes of 6 August 1977 near Springfield, Illinois. SMRP Res. Pap. No. 161, The University of Chicago, 50 pp. [NTIS PB 80-159791].

——, M. J. Markus and G. D. Lessens, 1980: Some synoptic and mesoscale factors associated with downburst-producing thunderstorms. *Preprints 8th Conf. Weather Forecasting and Analysis*, Denver, Amer. Meteor. Soc., 363–370.

Fujita, T. T., 1973: Tornadoes around the world. *Weatherwise*, **26**, 56–83.

——, 1974: Jumbo tornado outbreak of 3 April 1974. *Weatherwise*, **27**, 116–126.

——, 1975: Color map of superoutbreak tornadoes of 3–4 April 1974. *Weatherwise*, **28**, 55.

——, 1976a: History of suction vortices. *Proc. Symposium on Tornadoes*, Texas Tech. University, 78–88. [Available from Institute for Disaster Research, Box 4089 Tech Station, Texas Tech University, Lubbock, TX, 79409].

——, 1976b: Spearhead echo and downburst near the approach end of a John F. Kennedy Airport runway. SMRP Res. Pap. No. 137, The University of Chicago, 51 pp. [NTIS PB-254009]. See also Fujita and Byers (1977).

——, 1977: Anticyclonic tornadoes. *Weatherwise*, **30**, 51–64.

——, 1978: Manual of downburst identification for Project NIMROD. SMRP Res. Pap. No. 156, The University of Chicago, 104 pp. [NTIS PB-286048].

——, 1979: Objectives, operation, and results of Project NIMROD. *Preprints 11th Conf. Severe Local Storms*, Kansas City, Amer. Meteor. Soc., 259–266.

——, 1980: Downbursts and microbursts—An aviation hazard. *Preprints 19th Conf. Radar Meteorology*, Miami, Amer. Meteor. Soc., 94–101.

——, 1981: Tornadoes and downbursts in the context of generalized planetary scales. *J. Atmos. Sci.*, **38**, 1511–1534.

——, and H. R. Byers, 1977: Spearhead echo and downburst in the crash of an airliner. *Mon. Wea. Rev.*, **105**, 129–146.

——, and F. Caracena, 1977: An analysis of three weather-related aircraft accidents. *Bull. Amer. Meteor. Soc.*, **58**, 1164–1181.

——, and R. M. Wakimoto, 1981: Five scales of airflow associated with a series of downbursts on 16 July 1980. *Mon. Wea. Rev.*, **109**, 1438–1456.

——, D. L. Bradbury and C. F. Van Thullenar, 1970: Palm Sunday tornadoes of April 11, 1965. *Mon. Wea. Rev.*, **98**, 29–69.

Galway, J. G., 1981: Ten famous tornado outbreaks. *Weatherwise*, **34**, 100–109.

Golden, J. H., 1971: Waterspouts and tornadoes over south Florida. *Mon. Wea. Rev.*, **99**, 146–154.

——, 1974: Scale-interaction implications for the waterspout life cycle, II. *J. Appl. Meteor.*, **13**, 693–709.

——, and D. Purcell, 1977: Photogrammetric velocities for the Great Bend, Kansas, tornado of 30 August 1974: Accelerations and asymmetries. *Mon. Wea. Rev.*, **105**, 485–492.

——, and ——, 1978: Airflow characteristics around the Union City tornado. *Mon. Wea. Rev.*, **106**, 22–28.

Graham, H. E., 1955: Fire whirlwinds. *Bull. Amer. Meteor. Soc.*, **36**, 99–103.

Hubert, L. F., and A. F. Krueger, 1962: Satellite pictures of mesoscale eddies. *Mon. Wea. Rev.*, **90**, 457–463.

Huschke, R. E., Ed., 1959: *Glossary of Meteorology*. Amer. Meteor. Soc., 638 pp.

Idso, S. B., 1974: Tornado or dust devil: The enigma of desert whirlwinds. *Amer. Sci.*, **62**, 530–541.

——, 1975a: Observations of dust devils over water. *Bull. Amer. Meteor. Soc.*, **56**, 376.

——, 1975b: Whirlwinds, density currents, and topographic disturbances: a meteorological melange of intriguing interactions. *Weatherwise*, **28**, 61–65.

——, R. S. Ingram and J. M. Pritchard, 1972: An American haboob. *Bull. Amer. Meteor. Soc.*, **53**, 930–935.

Ingram, R. S., 1973: Arizona "eddy" tornadoes. NOAA Tech. Memo. NWS-WR-91, 9 pp. [NTIS COM 7410465].

Kelly, D. L., J. T. Schaefer, R. P. McNulty, C. A. Doswell III and R. F. Abbey, Jr., 1978: An augmented tornado climatology. *Mon. Wea. Rev.*, **106**, 1172–1183.

Lemon, L. R., 1976: Wake vortex structure and aerodynamic origin in severe thunderstorms. *J. Atmos. Sci.*, **33**, 678–685.

——, and C. A. Doswell III, 1979: Severe thunderstorm evolution and mesocyclone structure as related to tornadogenesis. *Mon. Wea. Rev.*, **107**, 1184–1197.

——, R. J. Donaldson, Jr., D. W. Burgess and R. A. Brown, 1977: Doppler radar application to severe thunderstorm study and potential real-time warning. *Bull. Amer. Meteor. Soc.*, **58**, 1187–1193.

——, C. A. Doswell, III, A. R. Moller and D. K. Hoadley, 1980: A slide series supplement to "Tornado: A Spotter's Guide." Available from National Audiovisual Center, Order Section, General Services Administration, Washington, DC 20409.

Lyons, W. A., and S. R. Pease, 1972: "Steam devils" over Lake Michigan during a January arctic outbreak. *Mon. Wea. Rev.*, **100**, 235–237.

Maddox, R. A., 1980: Mesoscale convective complexes. *Bull. Amer. Meteor. Soc.*, **61**, 1374–1387.

——, L. R. Hoxit and C. F. Chappell, 1980: A study of tornadic thunderstorm interactions with thermal boundaries. *Mon. Wea. Rev.*, **108**, 322–336.

Maxworthy, T., 1973: A vorticity source for large-scale dust devils and other comments on naturally occurring columnar vortices. *J. Atmos. Sci.*, **30**, 1717–1722.

Meaden, G. T., 1981: Whirlwind formation at a sea breeze front. *Weather,* **36,** 47–48.

Minor, J. E., J. R. McDonald and K. C. Mehta, 1977: Engineering-oriented examinations of the tornado phenomenon. *Preprints 10th Conf. Severe Local Storms,* Omaha, Amer. Meteor. Soc., 438–445.

Moller, A. R., 1978: The improved NWS storm spotters' training program at Ft. Worth, Texas. *Bull. Amer. Meteor. Soc.,* **59,** 1574–1582.

Novlan, D. J., and W. M. Gray, 1974: Hurricane-spawned tornadoes. *Mon. Wea. Rev.* **102,** 476–488.

Simpson, J. E., 1969: A comparison between laboratory and atmospheric density currents. *Quart. J. Roy. Meteor. Soc.,* **95,** 758–765.

Sinclair, P. C., 1969: General characteristics of dust devils. *J. Appl. Meteor.,* **8,** 32–45.

Testud, J., G. Breger, P. Amayenc, M. Chong, B. Nutten and A. Sauvaget, 1980: A Doppler radar observation of a cold front: Three-dimensional air circulation, related precipitation system and associated wavelike motions. *J. Atmos. Sci.,* **37,** 78–98.

Thorarinsson, S., and B. Vonnegut, 1964: Whirlwinds produced by the eruption of Surtsey volcano. *Bull. Amer. Meteor. Soc.,* **45,** 440–444.

Towery, N. G., and G. M. Morgan, Jr., 1977: Hailstripes. *Bull. Amer. Meteor. Soc.,* **58,** 588–591.

——, G. M. Morgan, Jr. and S. A. Changnon, Jr., 1976: Examples of the wind factor in crop-hail damage. *J. Appl. Meteor.,* **15,** 1116–1120.

Warn, G. F., 1952: Some dust storm conditions of the southern high plains. *Bull. Amer. Meteor. Soc.,* **33,** 240–243.

Williams, N. R., 1948: Development of dust whirls and similar small-scale vortices. *Bull. Amer. Meteor. Soc.,* **29,** 106–117.

Wilson, J., R. Carbone, H. Baynton and R. Serafin, 1980: Operational application of meteorological Doppler radar. *Bull. Amer. Meteor. Soc.,* **61,** 1154–1168.